Hindawi
Science and Technology of Nuclear Installations
Volume 2019, Article ID 8186798, 11 pages
https://doi.org/10.1155/2019/8186798

Research Article

Multilayer Shielding Design for Intermediate Radioactive Waste Storage Drums: A Comparative Study between FLUKA and QAD-CGA

Wenqian Li,[1] **Xuegang Liu**,[1] **Ming Li**,[2] **Yilin Huang**,[3] **and Sheng Fang**[1]

[1]*Institute of Nuclear and New Energy Technology, Collaborative Innovation Centre of Advanced Nuclear Energy Technology, Key Laboratory of Advanced Reactor Engineering and Safety, Ministry of Education, Tsinghua University, Beijing, 100084, China*
[2]*Nuclear and Radiation Safety Centre, Ministry of Environmental Protection of the People's Republic of China, Beijing, China*
[3]*Radiation-Environment Management and Monitoring Station of Guangxi Zhuang Autonomous Region, Guangxi, 530022, China*

Correspondence should be addressed to Sheng Fang; fangsheng@tsinghua.edu.cn

Received 17 December 2018; Revised 4 March 2019; Accepted 21 March 2019; Published 4 April 2019

Academic Editor: Michael I. Ojovan

To ensure that the outside dose rate of waste package is below the limitation of national laws and regulations, based on the standard 200L drum, a new drum with inner shielding was proposed for intermediate-level radioactive waste (ILW) storage. For comparison, FLUKA and QAD-CGA were used to verify the shielding design of the ILW storage drums produced in INET with multiple inner shielding layers. The flux and dose were calculated and analyzed for four different cases. In QAD-CGA calculation, it was found that different buildup factors can lead to the considerably different results. A weighted algorithm was proposed to correct QAD-CGA for multilayer shielding cases. In FLUKA calculation, parameter optimization and tailored variance reduction technique (VRT) were used. Quantitative efficiency evaluation of different FLUKA settings using the FOM factor was carried out. The differences in the calculated dose rates results between the FLUKA and QAD-CGA programs are within one order of magnitude. The results of QAD-CGA are generally higher than those of FLUKA. The analysis shows that appropriate corrections in QAD-CGA can make the trend of the calculation results more consistent with the theory. In FLUKA calculation, with optimized setting and VRT adopted, the calculation efficiency can be improved more than 20 times. The results of this study provide not only suggestions for the design of the ILW storage drums but also useful references for other similar work.

1. Introduction

While the nuclear power brings comfort and convenience to people's lives, it also produces radioactive waste inevitably. With the development of nuclear power and corresponding nuclear fuel cycle, the menace of radioactive waste has become increasingly prominent. At the end of 2010, the total volume of the low and intermediate-level radioactive waste (LILW) from nuclear power plants (NPPs) in China was about 10,000 cubic meters [1]. At present, the NPPs in China generate about 2,000 cubic meters of LILW per year. It is estimated that by 2020, the accumulation of these radioactive waste will reach 30,000 cubic meters [2]. Minimization of radioactive waste is one of the basic principles of radioactive waste management, which requires thorough and comprehensive considerations during the design to reduce the volume of radioactive waste as low as reasonably achievable (ALARA) [3, 4].

In China, the radioactive wastes are classified according to the Chinese national regulation into several categories, such as low-level waste (LLW), intermediate-level waste (ILW), and high-level waste (HLW) based on radioactive activity, half-life, decay type, and so on. The radioactive liquid waste generated during the operation and decommissioning stages of a nuclear facility is usually solidified into cement and then filled into the standard 200L steel drums.

There is a radioactive liquid waste cementation facility in the Institute of Nuclear and New Energy Technology (INET) of Tsinghua University (THU), located at Changping district, Beijing, China. The dominant contributor in the radioactive

waste is Cs-137 featured by the gamma radiation of 661.6 keV. After cementation, the waste in the drum is classified as ILW, which means a large amount of radioactivity inside the drum and a considerable radiation exposure outside the drum.

This work focuses on the shielding design of the ILW drum for storage. According to the Chinese regulations [5, 6], the maximum dose rate at the outer surface of the radioactive waste package (or container) shall not exceed the defined level during the storage, transportation, and final disposal of radioactive waste. For this purpose, some extra inner shielding layers made of cement [7] or other material [8] are usually introduced. If the thickness of inner shielding layer is not enough, the external dose of the drum will be too high; conversely, the loading capacity of waste will be reduced and the total number of waste drums will be increased. Therefore, an appropriate and optimized shielding design is significant, so that the waste loading capacity can be maximized and the outer radiation regulations can be followed. It will bring enormous benefits in terms of waste volume minimization, extra radiation protection simplification, and the resulting cost reduction.

In general, there are two approaches to perform such shield design: the Monte Carlo simulation method and the empirical formula approximation calculation method. For the former, FLUKA (http://www.fluka.org/fluka.php; [9]), MCNP [10], and GEANT4 [11] are all mature software currently used in the world for such a kind of Monte Carlo simulation calculations. And for the latter, QAD [12] is software developed based on the point-kernel integration technology by the Los Alamos National Laboratory and Oak Ridge National Laboratory, which can quickly perform the shielding calculation. The QAD-CGA is an improved version of the QAD by Wang et al. [13]. The Monte Carlo method will usually take an extremely long time to calculate, such as several days or even more for a complicated and elaborate model. By contrast, the empirical formula method will be easier and faster, but the accuracy is limited.

In recent years, many groups utilized the Monte Carlo methods and experimental validation to research the shielding design problem. For example, Suarez et al. [14] made the experimental measurements compared with Monte Carlo simulated results to test the shield design of a storage cask for HLW. However, the source term considered in Suarez's work is neutron of 2.5 MeV, which is different from this work's consideration, i.e., the photons with the energy lower than 661.6 keV.

Considering that the Monte Carlo software FLUKA has been verified by a lot of benchmark experiments and comparison calculation since developed time till recent years [15–18] and the QAD-CGA program is especially suitable for the radiation protection design and widely used in the reactor engineering [19–21], the FLUKA software with a version of 2011.2c and the QAD-CGA program were both adopted in the present study. The shielding calculation was performed for the standard 200L steel drums with inner shielding layers made of cement.

In this work, we put the emphasis on the comparison of the calculation methods and results. The FLUKA program has the advantage of accuracy, but it always takes a very long calculation time such as several days, even weeks. QAD-CGA has the advantage of rapid calculation, which may only take several seconds to a few minutes. However, the calculation results of QAD-CGA are usually less accurate and more conservative [22].

Compared with FLUKA, the QAD-CGA program adopts exponential decay and buildup factors to empirically describe the attenuation of gamma rays in different materials, instead of direct simulations of the complex photon-material interaction. In the QAD-CGA program, the radiation source volume will be discretized into a series of elementary cells, and the dose rate contribution by each cell will be calculated at different receiver points [23]. Therefore, QAD-CGA cannot calculate the energy spectrum of photon flux after the interaction and it assumes that the energy of photons at the receiver points remains the same as that of the radiation source.

The accuracy of the QAD-CGA calculation is related to the selection of the buildup factor [22, 24]. So the influence of buildup factors was studied, and a weighted related algorithm was proposed. In the FLUKA Monte Carlo simulation, the optimized parameter setting and the variance reduction technique (VRT) were applied for the improvement of the computational efficiency. The results of this study provide not only suggestions for the design of the ILW storage drums but also useful references for other similar work.

2. Materials and Methods

2.1. Parameters for Calculation

2.1.1. Geometry Models. The standard 200L steel drum is 56cm in diameter and 85cm in height, with a thickness of 1.2mm. The inner shielding layer was made of cement of 6 cm thickness. To shape the cement layer, an auxiliary support structure is needed, which is made of 1.0 mm stainless steel. An extra cement top cover is also needed for every drum to reduce radiation above the top.

Figure 1 is a photo taken from the top of one drum when the top cover was uncovered. Figure 2 is a photo for the auxiliary support structure placed upside down, which is made of stainless steel and should be manufactured before the cement watering. Figure 3 is the diagram for the cement top cover.

In this study, four cases were considered for the FLUKA and QAD-CGA calculation.

Case 1. Consider only the drum without inner shielding, and with an isotropic point source.

Case 2. The model of the drum is the same as Case 1, but the source is changed into a volume one with harmonious activity distribution. With these settings, the location and size of the source are consistent with the actual solidified radioactive waste.

Case 3. The model extends Case 2 by taking the cement inner shielding layer and the auxiliary support structure into consideration.

Table 1: The input parameters of source term in FLUKA and QAD-CGA.

parameters		values or descriptions
gamma energy (E_γ)		661.6 keV
gamma intensity (I_γ)		2.357E10 γ/s
characteristic and position	Case 1	isotropic point source, at the geometric center of the drum
	Case 2	harmoniously distributed volume source, at the actual position of cement solidified radioactive waste
	Case 3	
	Case 4	

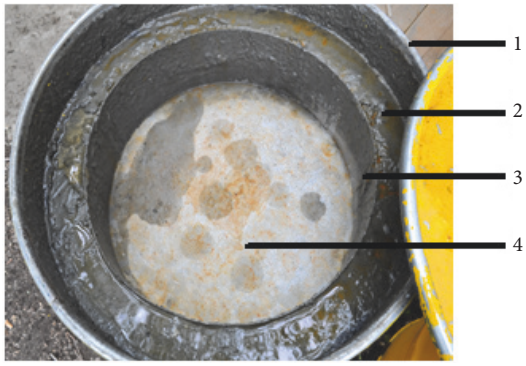

1. The standard 200L steel drum
2. the cement inner shielding layer
3. the auxiliary support structure
4. the cement solidified radioactive waste

Figure 1: A photo taken from the top of an ILW storage drum.

Figure 2: A photo for the auxiliary support structure.

Case 4. The cement solidified radioactive waste is added to the model of Case 3.

The above four cases are summarized in Figure 4.

2.1.2. Material Composition. The accuracy of the material composition may considerably impact the accuracy of the calculated results. In this work, the cement material composition was specially designed and tested for chemical and mechanical properties, which will not be introduced in this article. The compositions for different materials are listed in Figure 5.

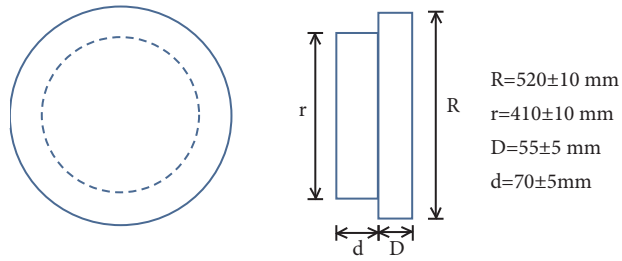

Figure 3: The diagram for the cement top cover.

2.1.3. Source Term. In this work, the waste comes from the spent nuclear fuel reprocessing process. The dominant contributors of radioactivity are Cs-137 and Sr-90 (>95% of the total activity). For the external exposure shielding design, only Cs-137 was taken into account.

The highest total activity of Cs-137 in an ILW storage drum is designed as 2.77E10 Bq. Since the highest energy of Cs-137 is 661.6 keV with a branching ratio of 85.1%, the corresponding gamma intensity (I_γ) will be 2.357E10/s.

In the FLUKA and QAD-CGA calculation, only the gamma ray of the highest energy was considered, while the gamma rays of lower energies were ignored. Since the shielding calculations are usually conservative, this simplification will not affect the estimation of the shielding effect. The input parameters of source term are summarized in Table 1.

2.1.4. Dose Conversion Factor. In this study, the ambient dose equivalent, H $*$ (10), was scored for the comparison and evaluation. The conversion coefficients are taken from the ICRP Publication 74 [25, 26].

2.2. Buildup Factors and Algorithm Improvement in QAD-CGA. In the QAD-CGA calculation, the buildup factor [22, 24] may considerably affect the results, which depends on the photon energy and shielding material [27]. QAD-CGA automatically chooses the buildup factor based on the energy of radiation source. In this study, a single buildup factor corresponding to 0.662 keV was adopted. For the material,

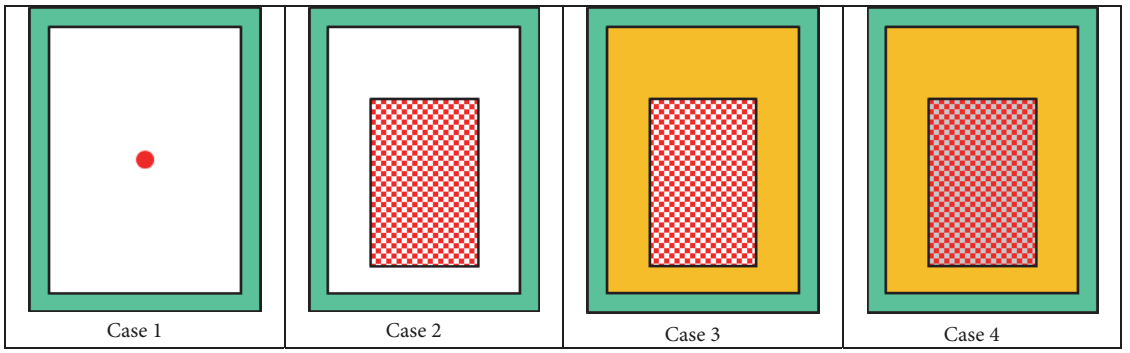

Figure 4: The four cases for the FLUKA and QAD-CGA calculation.

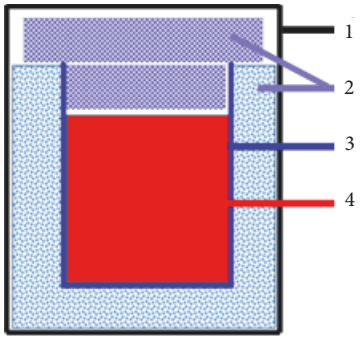

Material 1: carbon steel for the standard 200L steel drum

element	C	Mn	Si	Fe
%	0.15	0.3	0.25	99.3

Material 2: cement for the inner shielding layer and the top cover

component	SiO_2	Al_2O_3	CaO	Fe_2O_3
%	23.4	4.52	63.70	4.55
component	MgO	SO_3	TiO_2	H_2O
%	1.76	0.68	0.40	50

Material 3: stainless steel for the auxiliary support structure

element	Si	Cr	Ni	Mn	Fe
%	1	18	9	2	70

Material 4: cement for the solidified waste

component	SiO_2	Al_2O_3	CaO	Fe_2O_3	MgO
%	23.4	4.52	63.70	4.55	1.76
component	SO_3	TiO_2	H_2O	$NaNO_3$	
%	0.68	0.40	50	0.01	

Figure 5: The compositions for different materials.

QAD-CGA leaves the choice to the users. The selection of different buildup factors will affect the calculation of the scattered photons. In general, it is recommended to select the buildup factor according to the outermost layer material. But, only one type of materials can be chosen for determining the buildup factor in every calculation routine.

In this work, the comparison with FLUKA demonstrates that a careful selection of the buildup factors of the inner layer material can provide more reasonable results (detailed discussion in Section 3.2). This is because, in the case considered in this work, the thickness of outermost shield layer is very thin, and most of the shielding effect is contributed by the thicker inner shield material. In this case, if the buildup factor of the outermost material is still selected, the calculated dose distribution trend will deviate obviously from the actual situation. However, it is not acceptable to simply use the shielding factor of the inner layer material, because the calculated dose rate will be too high though the trend is better.

Thus, a weighted related algorithm was proposed for the dose (or dose rate) correction here. The calculation formula is as follows:

$$D = \sum_i W_i D_i, \tag{1}$$

$$\sum_i W_i = 1 \tag{2}$$

where D is the final dose (or dose rate) at the interesting point and W_i and D_i are the weight factor and the calculated dose (or dose rate), respectively, which corresponds to the buildup factor of material i.

In this work, since the thickness of the auxiliary support structure is very thin and can be neglected, formula ((1), (2)) can be simplified to ((3), (4)).

$$D = W_1 D_1 + W_2 D_2 \tag{3}$$

$$W_1 + W_2 = 1 \tag{4}$$

Here the subscripts 1 and 2 correspond to steel and cement, respectively.

The distribution of weight W_i should be related to the thickness of the shielding material. In addition, the outermost shielding material should also occupy a higher weight. Under this consideration, the following three groups of weights are proposed and compared in Section 3.

① $W_1 = 0.25$,

$W_2 = 0.75$

Table 2: The cutoff energy and Russian roulette splitting setting.

regions	cutoff energy	splitting number
(1) the standard 200L steel drum	1 keV	4
(2) the cement inner shielding layer	9 keV	2
(3) the auxiliary support structure	9 keV	2
(4) the cement solidified radioactive waste	80 keV	-

$$\begin{aligned} &② \; W_1 = 0.50, \\ &\quad W_2 = 0.50 \\ &③ \; W_1 = 0.75, \\ &\quad W_2 = 0.25 \end{aligned} \tag{5}$$

2.3. Optimized Setting and Variance Reduction Technique in FLUKA. For the Case 4's geometry model, the self-absorption of the cement solidified waste can greatly increase the calculation time in the FLUKA simulation. To avoid this problem, an improved input file was also executed with the optimized setting and VRT adopted. The calculation results and efficiency of the optimized setting and VRT will be compared with those of the direct input and discussed in Section 3.

The optimized setting adopts different cutoff energies for different regions. It is under the following assumption: if the transported particle cannot go out from the inner layer with enough energy, it will eventually have very low chance to get out of the outermost one, and the transport of the particles will be just stopped in the current layer.

Specifically, the VRT used in this work is setting higher importance for outer regions, which is based on the Russian splitting skill: if a transported particle goes into the region with splitting number N, the particle will split into N particles and every split particle will have the weight of 1/N.

The cutoff energy and splitting setting for every region are listed in Table 2.

2.4. Definition and Description for Flux Comparison. In this problem, the photons emitted by C-137 will react with matters. Some of the photons penetrate the shielding layers, while other photons undergo reactions such as electromagnetic shower. In this way, the number of photons with low energies will increase. Since QAD-CGA program does not consider the attenuation of photon energy, the flux spectra at points of interest were only calculated by the FLUKA program.

A comparison of the fluxes at points of interest between the four cases can clearly provide a judgment about the rationality and correctness of the FLUKA calculation. For this purpose, two quantities are defined as follows:

N_E represents the number of the total energy photons in the flux, which penetrate all shielding layers without any reaction.

N_T represents the total number of photons in the flux, including not only directly penetrating photons, but also scattered photons and the secondary photons.

For an isotropic point source, if there is no shielding, the attenuation of the flux will follow the formula

$$\Phi_R = \frac{\Phi_0}{4\pi R^2} \tag{6}$$

where Φ_R is the flux at a distance of R and Φ_0 is equal to the gamma intensity I_γ of the source.

For Case 1, the comparison between N_E, N_T, and Φ_R can provide a check of the accuracy of the primary FLUKA calculation. Since the thickness of the drum is very thin, the difference between these three quantities should not be very large.

Similarly, for the other cases, N_E and N_T should have a reasonable and bounded variation compared with the former case. In this way, the accuracy of the calculation can be verified.

2.5. FOM Factor for Efficiency Comparison. The Figure-of-Merit (FOM) factor [28] is adopted usually to evaluate the computational efficiency of the Monte Carlo method, which can be calculated by

$$FOM = \frac{1}{R^2 T} \tag{7}$$

where T is the total time needed by a calculation and R is the relative uncertainty. If the calculation is performed in parallel, T should be the sum of parallel computing time. The higher the value of the FOM factor is, the higher the computational efficiency of the method is.

3. Results and Discussion

3.1. Fluxes. Because the QAD-CGA program is not able to provide the resultant flux, this section only discusses the flux results of FLUKA.

For the flux scoring, two detectors were set at the top and side of the ILW storage drums, respectively. The top detector is pie-shaped, covering all the top area with 1cm of height. The side detector is ring-shaped, covering only the middle of the side area with 1cm of height. Figure 6 shows the positions of the two detectors.

The flux results listed in this section are all corresponding to one primary photon. Figure 7 shows the flux results for the four cases. The FLUKA calculation can provide the error statistics, which are also included in the figures.

As defined and described in Section 2.4, the three quantities (N_E, N_T, Φ_R) of the four cases were summarized in Table 3.

For Case 1, the values of N_E/Φ_R, which represent the ratio of photons that penetrated the shielding directly compared with no shielding, are 56% and 69%, respectively, for top and side detectors. The values of N_E/N_T, which represent

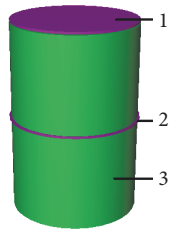

1. top detector
2. side detector
3. storage drums

Figure 6: The positions of the two flux detectors.

Table 3: Summarization of N_E, N_T, and Φ_R of the four cases.

Quantities		Fluxes (1/cm^2/p)		
		top	side	average[c]
Φ_R		4.41E-05	1.02E-04	7.31E-05
N_E	Case 1	2.48E-05	7.03E-05	4.76E-05
	Case 2	4.99E-05	4.97E-05	4.98E-05
	Case 3	1.23E-05	1.81E-05	1.52E-05
	Case 4 [a]	2.30E-06	4.65E-06	3.48E-06
	Case 4 [b]	2.30E-06	4.64E-06	3.47E-06
N_T	Case 1	2.81E-05	7.68E-05	5.25E-05
	Case 2	5.52E-05	5.49E-05	5.51E-05
	Case 3	3.00E-05	4.17E-05	3.59E-05
	Case 4 [a]	7.68E-06	1.98E-05	1.37E-05
	Case 4 [b]	7.68E-06	1.98E-05	1.37E-05

a: direct calculation.
b: optimized setting and VRT adopted.
c: the average value of the top and side values.

the proportion of total energy photons outside of the drum compared with all photons, are 88% and 91%, respectively, for top and side detectors. Since the area of the top detector is larger than the side detector, more photons will go through the top shielding layer obliquely. So the probability of reaction will be larger for the top direction than the side. In this way, the values of N_E, N_T, N_E/Φ_R, and N_E/N_T for the top should all be lower than the side. The calculation results are also consistent with the above analysis.

For Case 2, the N_E and N_T average values of the top and side are quite close to the results of Case 1. This is because the intensity of the two sources is equal though the shapes are different. As can be seen from Figure 7, the flux spectra of the side and top are more consistent compared with Case 1, because the uniformly distributed source reduces the difference between the top and sides. The values of N_E/N_T for top and side are both 90%, which are also close to Case 1's results. However, contrary to Case 1, the top values of N_E and N_T are slightly higher than the side ones. This is because the axial height of the drum is larger than the diameter, which increases the number of photons in the vertical direction.

For Case 3, due to the effect of the inner shielding layer, N_E and N_T are obviously lower than the value of Case 2. And the N_E/N_T ratios for top and side decreased to 41% and 43%. This shows that many photons react with the shielding. Contrary to Case 2, the top values of N_E and N_T are lower than the side ones. This is because the cement top cover has a thickness of 12.5 cm (Figure 3), which is much higher than 6 cm on the side.

For Case 4, two inputs were used: (A) direct calculation; (B) optimized setting and VRT adopted. The flux spectra are quite similar in the high energy region for (A) and (B). But in the low energy region, due to the setting of energy cutoff in (B), there are some deviations between the two results, and the statistical uncertainty of (A)'s results is larger than (B)'s. However, these deviations will not have a significant effect on the dose calculation (see Section 3.2 for details). Also, the results of N_E and N_T are quite close for (A) and (B). Compared with Case 3, the values of N_E and N_T are further reduced, which is due to the effect of self-absorption. And the ratios of N_E/N_T decreased to 30% and 23% for the top and side. Similar to Case 3, the top values of N_E and N_T are much lower than the side ones, which is also related to the self-absorption of the cement solidified radioactive waste.

In the all flux graphs a sharp peak appears at energy range of 6.2 to7.8 keV; this corresponds to the characteristic X-rays of iron.

3.2. Dose Rates. The dose rates given in this section are all scaled with the total gamma intensity in Section 2.1.3.

3.2.1. 3D Dose Rate Distribution by FLUKA. The FLUKA program provides the three-dimensional dose rate calculation results. The corresponding statistical error for each data point will also be calculated. By increasing the number of simulated particles, statistical errors can be reduced. In this work, the error is controlled under 3%. The software SimpleGeo (http://www.fluka.org/fluka.php) is used to display the three-dimensional data matrix in a 3D view.

Figure 8 shows the 3D dose rate distribution for Case 3. As can be seen from Figure 8, for Case 3, the dose rate on the side of the drum is approximately 7 to 12 mSv/h.

Figure 9 gives the comparison of front views of the dose rate distributions for Case 4 by direct calculation method and by optimized calculation method (refer to Section 2.3). As can be seen from the figure, the difference in the calculation results is very small. Two small disagreements are marked out by red circles in Figure 9, which are caused by the cutoff energy setting.

For comparison, Figure 10 summarizes the dose rates calculated by FLUKA at two points of interest for the four cases.

3.2.2. QAD-CGA Calculated Dose Rates. The QAD-CGA program typically only provides the dose results for the point of interest instead of the 3D dose distribution. Here the top and side surface midpoints of the drum are selected as points of interest, as shown in Figure 10. Figure 10 lists the dose rates for the two points of interest calculated by QAD-CGA as well as by FLUKA.

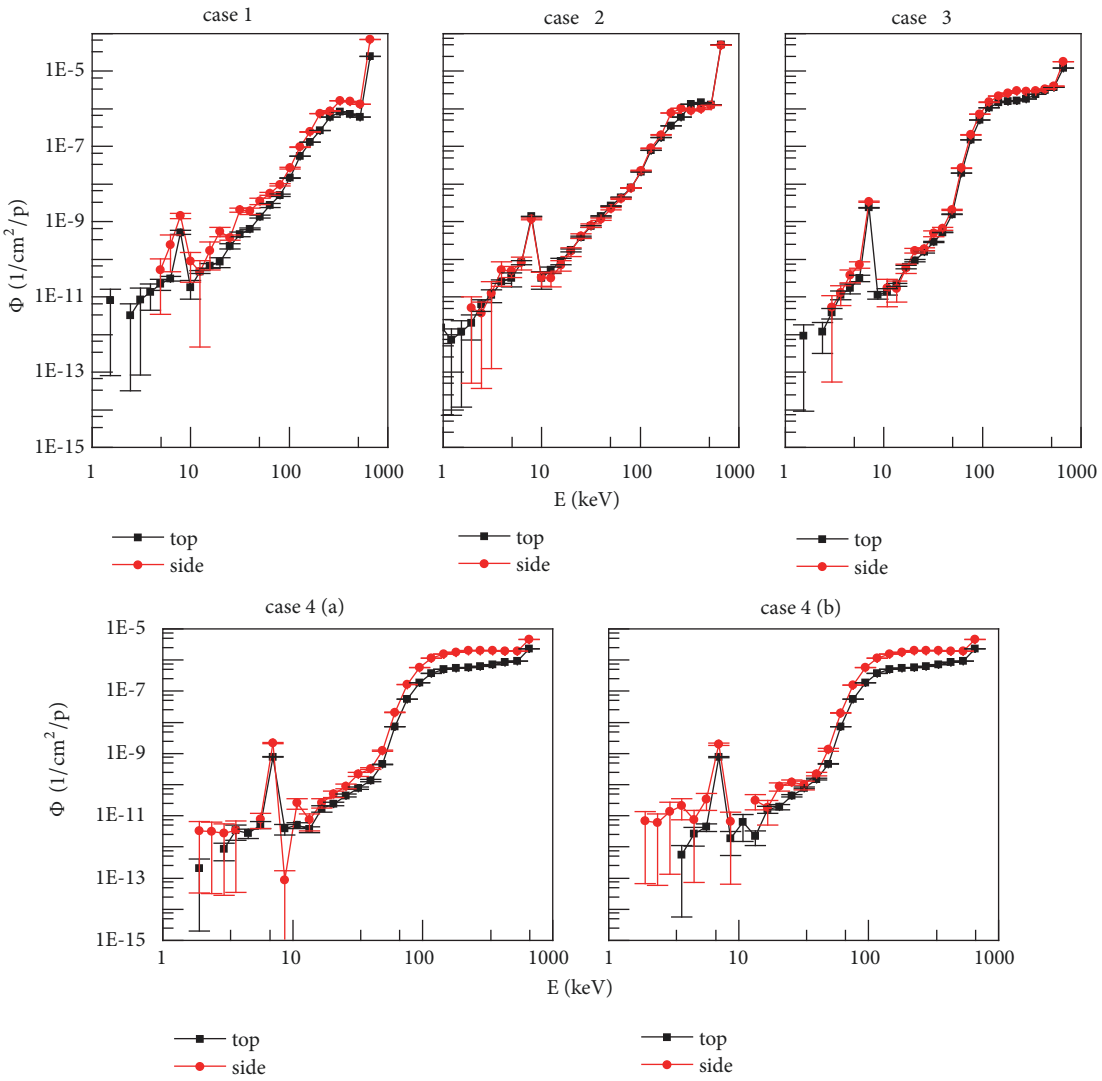

FIGURE 7: FLUKA-calculated flux results for the four cases. Case 4 (a): direct calculation. Case 4 (b): optimized setting and VRT adopted.

As can be seen from Figure 10, for Cases 1 and 2, the results given by FLUKA and QAD-CGA agree very well, with F/Q values ranging from 48% to 73%.

For Case 1, the results by the two methods both indicate that the dose rate at the P1 point will be higher than P2's value. This can be explained by the fact that the P1 point is located closer to the source than P2.

For Case 2, the results by the two methods both indicate that the dose rate at the P1 point will be lower than P2's value. This is because a homogeneous distributed volume source was adopted in Case 2, and the height of the source is higher than the diameter. The height direction will contribute more to the dose rate without considering the self-absorption.

For Cases 1 and 2, the results of both FLUKA and QAD-CGA calculations are consistent with the theoretical analysis.

However, for Case 3, the situation became more complicated: the FLUKA-calculated dose rate at P1 is slightly lower than at P2, for the same reason as Case 2. However, in the QAD-CGA calculation, when the buildup factor of iron is used, the dose rate at P1 is higher than at P2, which is contrary to the FLUKA result, while when the buildup factor of cement is used, the dose rate at P1 is lower than at P2, which is the same as the FLUKA result. Case 4 is similar to Case 3: the calculated results show a more consistent trend with FLUKA by using the buildup factor of cement. And as can be seen from Figures 8 and 9, the dose distributions given by FLUKA are reasonable.

This phenomenon indicates that the prediction of the dose distribution trend will deviate from the actual situation if only the buildup factor of the outermost material is adopted.

Besides, for Cases 3 and 4, it should also be noted that with the buildup factor of cement adopting, the corresponding F/Q values are lower. This means that if the buildup factor of cement is used, the results given by QAD-CGA will be more conservative.

In order to improve the calculation results of QAD-CGA, Section 2 proposes a weighted related correction algorithm.

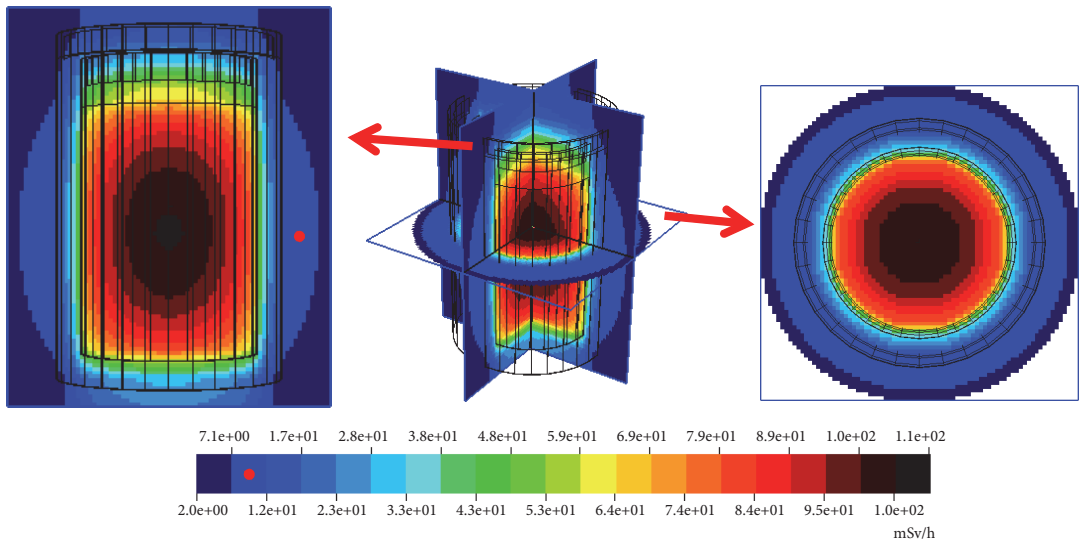

Figure 8: FLUKA-calculated 3D dose rate distribution for Case 3.

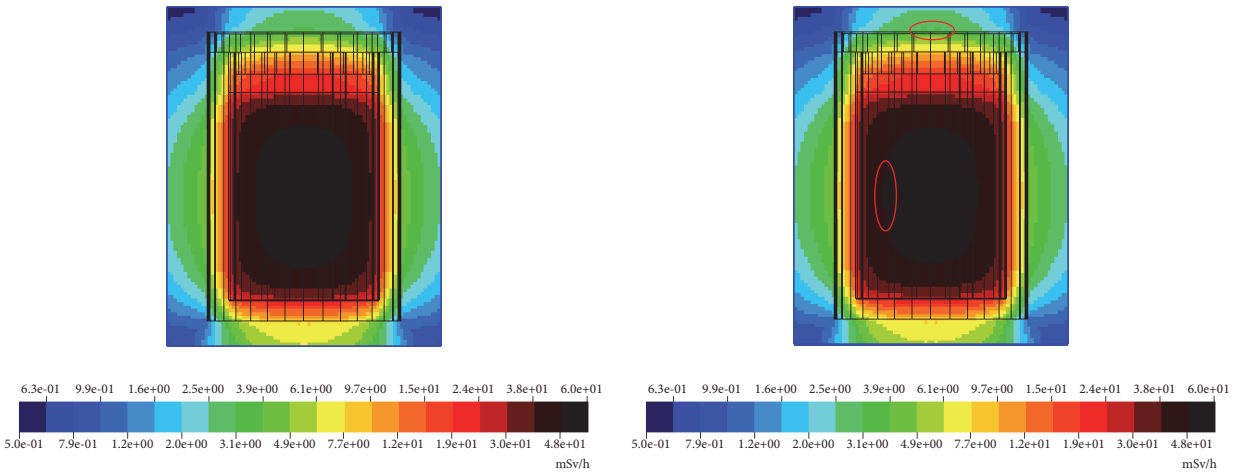

(a) Direct calculation (b) Optimized calculation

Figure 9: The front views of the dose rate distributions for Case 4 by direct (a)/optimized (b) calculation method.

The results of Cases 3 and 4 were corrected according to the three groups of weights listed in (5) and compared with the results of FLUKA. The results are shown in Figure 11.

As can be seen from the results, appropriate corrections can make the trend better. For Cases 3 and 4, using the ② group weights, the trend of QAD-CGA calculation results can be more consistent with FLUKA.

3.2.3. Comparison and Discussion for Dose Rates. In Figure 10, the F/Q value is the ratio of the FLUKA and QAD-CGA calculated dose rates. The F/Q values range from 0.13 to 0.73 for all cases, indicating that the differences of calculated dose rates by the FLUKA and QAD-CGA programs are within one order of magnitude. In addition, the QAD-CGA results are generally higher than FLUKA, so QAD-CGA is more conservative. By using different buildup factors, the results will be influenced. Appropriate corrections can make the trend of the calculation results more consistent with the theory.

3.3. Calculation Efficiency Comparison. The calculation of QAD-CGA is usually done immediately, and the waiting time will be no more than a few minutes which can be ignored, while the FLUKA calculation is usually more time-consuming.

The calculation cost and efficiency of FLUKA are summarized in Table 4, from which it can be seen that the calculation efficiency of the direct calculation method is very low for

		units	P1	P2
Case1	FLUKA	mSv/h	26.9	12.1
	QAD-CGA	mSv/h	42.5 (a)	18.7 (a)
	F/Q values	-	*0.63*	*0.65*
Case2	FLUKA	mSv/h	18.6	30.7
	QAD-CGA	mSv/h	38.7 (a)	41.8 (a)
	F/Q values	-	*0.48*	*0.73*
Case3	FLUKA	mSv/h	10.2	12.3
	QAD-CGA	mSv/h	22.9 (a) 42.0 (b)	17.0 (a) 51.3 (b)
	F/Q values	-	*0.45* (a) *0.24* (b)	*0.72* (a) *0.24* (b)
Case4	FLUKA	mSv/h	3.9	2.9
	QAD-CGA	mSv/h	5.7 (a) 30.9 (b)	12.2 (a) 16.4 (b)
	F/Q values	-	*0.68* (a) *0.13* (b)	*0.24* (a) *0.18* (b)

(a) Calculated with the buildup factor of iron
(b) Calculated with the buildup factor of cement

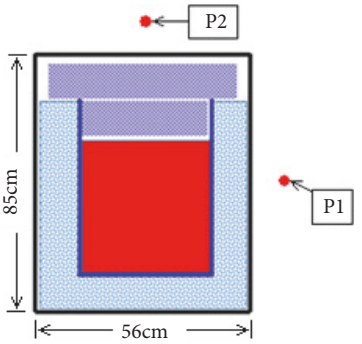

P1 and P2 are respectively 2 cm/ 2.5 cm from the center of the side and top surface.

Figure 10: Calculated dose rates at the two points of interest by FLUKA and QAD-CGA, and the FLUKA's results compared to the QAD-CGA's (F/Q values).

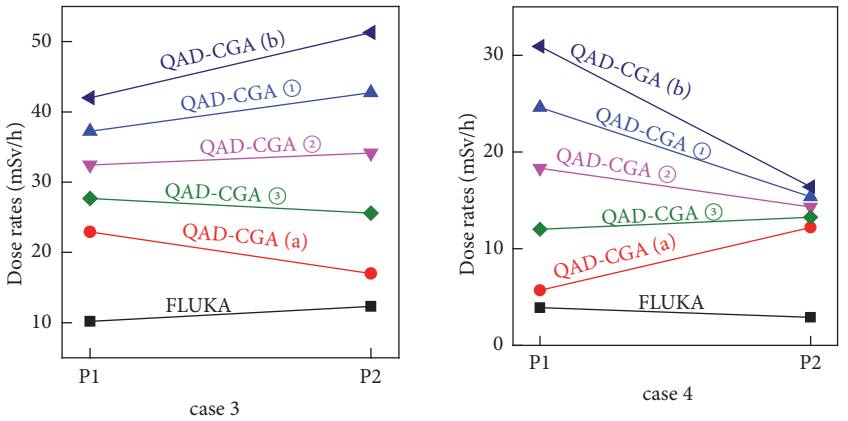

QAD-CGA (a): Calculated with the buildup factor of iron
QAD-CGA ①: Corrected with the ① group weights in equation (5)
QAD-CGA ② Corrected with the ② group weights in equation (5)
QAD-CGA ③ Corrected with the ③ group weights in equation (5)
QAD-CGA (b): Calculated with the buildup factor of cement

Figure 11: The corrected results of Cases 3 and 4 with the three groups of weights listed in equation (5) and comparison with other results.

Table 4: Comparison of the calculation cost and efficiency of FLUKA.

	Total time	Average CPU time for a primary particle	Total number of particles	Parallel number	Error[c]	FOM factor (1/s)
Case 1	4.625 h	1.67E-04s	1E8	1	0.62%	1.56
Case 2	25.5 h	1.84E-04s	5E8	1	0.33%	1.00
Case 3	5 d	2.16E-03	1.00E+09	5	0.44%	0.024
Case 4 [a]	9 d	3.70E-03	1.80E+09	9	0.53%	0.005
Case 4 [b]	25.6 h	9.23E-04	1.00E+08	1	0.98%	0.11

a: direct calculation.
b: optimized setting and VRT adopted.
c here gives the maximum statistical relative error of the dose calculation matrix.

Cases 3 and 4, while when the optimized setting and VRT are adopted, the calculation efficiency is greatly improved. The FOM factor of Case 4 (b) is more than 20 times that of Case 4 (a).

4. Conclusions

The FLUKA and QAD-CGA programs were used for the shielding calculation of the ILW storage drums which are manufactured in the INET of Tsinghua University. The accurate material composition and geometry models were taken into consideration. The flux and dose for four different cases were calculated and compared.

In QAD-CGA calculation, it is recommended to select the buildup factor according to the outermost layer material and only one buildup factor can be set in every calculation routine. In this work, the comparison with FLUKA demonstrates that a careful selection of the buildup factors of the inner layer material can provide more reasonable results. So a weighted correction algorithm was proposed for multilayer shielding. The analysis shows that appropriate corrections can make the trend of the calculation results more consistent with the theory.

In FLUKA calculation, parameters optimization and tailored variance reduction technique (VRT) were used. The FLUKA-calculated flux results of four different cases were compared and analyzed in detail, which shows that the FLUKA calculation of flux is reasonable. Quantitative efficiency evaluation of different FLUKA settings using the FOM factor was carried out. A comparison shows that, with the optimized setting and VRT, the calculation efficiency can be improved more than 20 times, while the difference of the calculation results compared to the direct method is very small.

By comparison, the differences in the calculated dose rates results between the FLUKA and QAD-CGA programs are within one order of magnitude. The results of QAD-CGA are generally higher and more conservative than those of FLUKA.

Data Availability

The data used to support the findings of this study are available from the corresponding author upon request.

Conflicts of Interest

The authors declare that they have no conflicts of interest.

Acknowledgments

This work is supported by the National Natural Science Foundations of China [grant number 11875037 and grant number 11475100] and the foundation of Key Laboratory of Advanced Reactor Engineering and Safety, Ministry of Education [grant number ARES-2018-08].

References

[1] W. T. Zheng and X. J. Cheng, "Research on related problems of low and intermediate level radioactive waste disposal in China," *Energy Construction*, vol. 1, no. 1, pp. 75–82, 2014 (Chinese).

[2] F. G. Liu, L. P. Liu, F. F. Dong et al., "Discussion on the minimization of radioactive waste of the nuclear power plants in China," *Nuclear standard measurement and quality*, 2018 (Chinese).

[3] IAEA., *Considerations for Waste Minimization at the Design Stage of Nuclear Facilities*, vol. 460, 2007.

[4] "U.S. Nuclear Regulatory Commission, Regulatory Guide 4.21: Minimization of Contamination and Radioactive Waste Generation: Life-Cycle Planning," 2008.

[5] GB11806, "Radioactive material safe transport regulations," *Chinese National Standards*, 2004.

[6] GB14500, "Radioactive waste management regulations," *Chinese National Standards*, 2002.

[7] H. Q. An, "Analysis and research on the key difficulties in supervision of the no. 105 decommissioning projects," *Urban Construction Theory Research*, vol. 3, pp. 110-111, 2018 (Chinese).

[8] Z. Jiang, C. Li, D. Li et al., "Medium radioactivity-level technology waste temporary storing shielding container, has bucket body formed with inner shielding layer, and header fixed with steel shell that is filled with lead sand shielding layer," *CN204966066-U*, 2016.

[9] A. Ferrari, P. Sala, A. Fasso, and J. Ranft, "FLUKA: a multi-particle transport code," CERN-2005-010, INFN TC_05/11, SLAC-R-773, 2008.

[10] D. B. Pelowitz, "MCNPX User's Manual," Version 2. 6. 0. Los Alamos National Laboratory Report LA-CP-07-1473, 2008.

[11] S. Agostinelli et al., "Geant4a simulation toolkit," *Nuclear Instruments and Methods in Physics Research Section A*, vol. 506, pp. 250–303, 2003.

[12] R. E. Malenfant, *QAD: A Series of Point-Kernel General Purpose Shielding Programs*, Los Alamos Scientific Lab., New Mexico, USA, 1966.

[13] W. Y. Wang, L. G. Zhang, J. Z. Cao, and F. Xie, "Optimization of the radiation shielding program QAD," in *Proceedings of the 2016 24th International Conference on Nuclear Engineering*, Charlotte, NC, USA, 2016.

[14] H. S. Suárez, F. Becker, A. Klix, B. Pang, and T. Döring, "Neutron flux measurements on a mock-up of a storage cask for high-level nuclear waste using 2.5 MeV neutrons," *Journal of Radiological Protection*, vol. 38, no. 3, pp. 881–891, 2018.

[15] E. Gschwendtner, C. W. Fabjan, N. Hessey, T. Otto, and H. Vincke, "Measuring the photon background in the LHC experimental environment," *Nuclear Instruments and Methods in Physics Research Section A: Accelerators, Spectrometers, Detectors and Associated Equipment*, vol. 476, no. 1-2, pp. 222–224, 2002.

[16] R. Tayama, H. Handa, K. Hayashi et al., "Benchmark calculations of neutron yields and dose equivalent from thick iron target for 52-256 MeV protons," *Nuclear Engineering and Design*, vol. 213, no. 2-3, pp. 119–131, 2002.

[17] L. Sihver, D. Mancusi, K. Niita et al., "Benchmarking of calculated projectile fragmentation cross-sections using the 3-D, MC codes PHITS, FLUKA, HETC-HEDS, MCNPX_HI, and NUCFRG2," *Acta Astronautica*, vol. 63, no. 7-10, pp. 865–877, 2008.

[18] E. Iliopoulou, P. Bamidis, M. Brugger et al., "Measurements and FLUKA simulations of bismuth and aluminium activation at the CERN Shielding Benchmark Facility (CSBF)," *Nuclear Instruments and Methods in Physics Research Section A: Accelerators, Spectrometers, Detectors and Associated Equipment*, vol. 885, Article ID WOS:000424740800010, pp. 79–85, 2018.

[19] W. Q. Li, S. Fang, and H. Li, "Research on the induced radioactivity of HTR-PM's reactor pressure vessel: A comparative study between FLUKA, KORIGEN and QAD-CGA," *Annals of Nuclear Energy*, vol. 114, pp. 129–135, 2018.

[20] S. Fang, H. Li, and W. Li, "Radiation protection calculation and optimization for shielding design around the refueling pipelines of HTR-PM," in *Proceedings of the 2018 26th International Conference on Nuclear Engineering*, p. V007T10A024, ICONE26, London, UK, 2018.

[21] S. Fang, H. Li, J. Cao, W. Li, F. Xie, and J. Tong, "γ dose rate estimation and operation management suggestions for decommissioning the reactor pressure vessel of HTR-PM," in *Proceedings of the ASME 2013 15th International Conference on Environmental Remediation and Radioactive Waste Management, ICEM 2013*, ICEM, Belgium, September 2013.

[22] J. K. Shultis and R. E. Faw, "Radiation shielding technology," *Health Physics Journal*, vol. 88, no. 4, pp. 297–322, 2005.

[23] M. Prokhorets, II. Prokhorets, S. Khazhmuradov et al., "Point-Kernel method for radiation fields simulation," *Problems of atomic science and technology*, vol. 48, 2007.

[24] Y. Harima, "An historical review and current status of buildup factor calculations and applications," *Radiation Physics and Chemistry*, vol. 41, no. 4-5, pp. 631–672, 1993.

[25] ICRP Publication 74, "Conversion coefficients for use in radiological protection against external radiation," *International Commission on Radiological Protection*, 1996.

[26] M. Pelliccioni, "Overview of fluence-to-effective dose and fluence-to-ambient dose equivalent conversion coefficients for high energy radiation calculated using the fluka code," *Radiation Protection Dosimetry*, vol. 88, no. 4, pp. 279–297, 2000.

[27] V. P. Singh and N. M. Badiger, "Comprehensive study of energy absorption and exposure build-up factors for concrete shielding in photon energy range 0.015-15 MeV up to 40 mfp penetration depth: Dependency of density, chemical elements, photon energy," *International Journal of Nuclear Energy Science and Technology*, vol. 7, no. 1, pp. 75–99, 2012.

[28] T. Shi, J. Ma, H. Huang, Y. Qiu, Z. Li, and D. Qian, "A new global variance reduction technique based on pseudo flux method," *Nuclear Engineering and Design*, vol. 324, pp. 18–26, 2017.